Crystal chemistry and ab initio investigations of new hard tetragonal C9 and C12 allotropes with edge- and corner-sharing C4 tetrahedra and diamond-related properties

Samir Matar, Vladimir Solozhenko

Crystal chemistry and *ab initio* investigations of new hard tetragonal C_9 and C_{12} allotropes with edge- and corner-sharing *C4* tetrahedra and diamond-related properties

Samir F. Matar [1,*] and Vladimir L. Solozhenko [2]

[1] Lebanese German University (LGU), Sahel Alma, Jounieh, Lebanon
https://orcid.org/0000-0001-5419-358X

[2] LSPM–CNRS, Université Sorbonne Paris Nord, 93430 Villetaneuse, France
https://orcid.org/0000-0002-0881-9761

Abstract

Stable tetragonal C_9 and C_{12} with original topologies have been devised based on crystal chemistry rationale and unconstrained geometry optimization calculations within the density functional theory (DFT). The two new carbon allotropes are characterized by corner- and edge-sharing tetrahedra, they are mechanically (elastic constants) and dynamically (phonons) stable, and exhibit thermal and mechanical properties close to diamond. The electronic band structures show insulating behavior with band gaps close to 5 eV, similar to diamond.

Keywords: carbon allotropes; DFT; crystal structures; mechanical properties; phonons; heat capacity; electronic band structures

* Corresponding author (e-mail: s.matar@lgu.edu.lb)

Introduction

Intensive research efforts are currently underway to identify novel carbon allotropes with the goal of achieving specific mechanical and thermal properties approaching those of diamond. For this purpose, modern materials research programs based on evolutionary crystallography are used to predict novel allotropes [1]. Regarding the carbon database, SACADA [2] is recognized as a reliable one available to all researchers. The novel allotropes are subjected to topology analysis using TopCryst software [3] and then published in the Cambridge Structural Database (CCDC). Despite the help provided by AI in generating carbon stoichiometries and structures, the role of the physicist and chemist remains essential, especially in the crystal chemistry that underlies structural engineering.

To illustrate this approach, and keeping in mind the *C4* tetrahedron building block of diamond, a simple arrangement of 8 *C4* tetrahedra at a cube corner and center is shown in Fig. 1a, with both ball-and-stick and tetrahedral representations exhibiting corner-sharing tetrahedra. The resulting body-centered tetragonal (bct) structure C_4 submitted to quantum mechanical calculation within the Density Functional Theory (DFT) [4,5] to obtain the ground state energy and related properties was found to be another formulation of diamond, and the allotrope is qualified with **dia** topology (Table 1) [6]. Using bct C_4 as a template, we devised novel simple allotropes, such as the latest one: hybrid (sp^3/sp^2) C_6 with **tfa** topology, which we called "neoglitter" (cf. [7] and the works cited therein).

Within a similar approach, we propose herein two novel carbon allotropes, tetragonal C_9 and C_{12}, both characterized by sp^3 carbon in original architectures comprising corner and edge sharing tetrahedra. The purpose of this paper is to present their crystal structures and to demonstrate ultrahardness, while also presenting high phonon optical mode frequencies of $\omega > 40$ THz like in diamond and C_4, a large electronic band gap, and a temperature evolution of the heat capacity close to that of diamond.

Computation framework

The computational methodology was developed in previous works [8,9]. Essentially, the search for the ground state structures with minimal energies was systematically performed using unconstrained geometry optimizations within the DFT-based Vienna Ab initio Simulation Package (VASP) [9,10] using the projector augmented wave (PAW) method for potentials [10]. The DFT exchange-correlation (XC) effects were treated using a generalized gradient approximation (GGA) [11]. The plane wave energy cut-off was 500 eV. The study of the mechanical properties was based on the calculations of the elastic properties, which were determined by performing finite distortions of the lattice and deriving the elastic constants from the strain-stress relationship. The calculated elastic constants C_{ij} are then used to obtain the bulk (B) and the shear (G) moduli with the Voigt averaging method [12] based on uniform strain. In addition to the mechanical properties, the dynamic stability was determined from the phonons, which are described as vibrational quanta. They are represented by phonon band structures obtained using the interface code "Phonopy" based

on the Python language [13]. The representations of the structures and charge density projections were obtained with the graphical program VESTA [14]. For the evaluation of the electronic properties the band structures were obtained with the all-electrons augmented spherical wave method ASW [15].

Crystal chemistry

The crystal parameters of the template bct C_4 (*I*-4*m*2, No. 119) are given in Table 1. We adopt an original method to introduce novel allotropes. The protocol consists of removing the central carbon, resulting in a simple tetragonal C_3 (*P*-4*m*2, No. 115). The central void can then accommodate the inserted carbon atoms in an enlarged cell.

The insertion of two sets of four-fold (4i) and (4j) occupations in the same space group leads to the C_9 stoichiometry. The geometry optimization down to the ground state energies through successive calculation cycles with increasing precision of the tetragonal Brillouin zone led to the lattice parameters and energies given in Table 1, 2nd column. In Fig. 1b, the structure of C_9 in both the ball-and-stick and tetrahedral representations shows similar, though larger, tetragonal C_4 with tetrahedra at corner site (shown as brown and white spheres) at the 8 corners connected by C2(4j) (white spheres). C3(4i) at z = ½ forming the central square (green spheres) are connected to C2 to form two edge-sharing tetrahedra (Table 1). As the original occurrence, the structure then consists of both corner and edge sharing tetrahedra. Note that the tetrahedra are significantly distorted, as can be seen from the angles.

Starting from the square configuration of C_9 with C3(4i) at x,x,½ transformed to C1(4h) at x,x,0 (brown spheres), the structure was completed with C2(8i) (white spheres) and removal of the corner atoms, then subjected to full geometry optimization. The crystal data are given in Table 1. The structure of C_{12} shown in Fig. 1c now consists only of edge-sharing *C4* tetrahedra.

The CIFs (crystal information files) of two structures were submitted to topology studies performed with the TopCryst program [3]. While C_4 used as template is designated with **dia** topology, C_9 was assigned with "4,4,4**T**6902-**HZ**" topology, and C_{12} was identified with "**sqc**5532" topology. We note here that there are three allotropes with **sqc** topology in the SACADA database: **sqc**1427 (space group No. 125), No. **sqc**3051 (space group No. 114), and **sqc**6952 (space group No. 133) [2]. The first two contain sp^2 carbon, while the third one shows only tetrahedral C(sp^3) with corner sharing tetrahedra. Structures with carbon squares are documented in the SCACADA database as **crb** topology with bct space groups (cf. No. 60-64 [2]). The novel C_9 and C_{12}, not cataloged in databases, were subsequently deposited, curated, and then deposited in CCSD: C_9 and C_{12} [17].

From the densities, the diamond-like C_4 structure is found to have the highest density, i.e. $\rho(C_4) = 3.50$ g/cm^3 versus $\rho(C_9) = 2.92$ g/cm^3, and $\rho(C_{12}) = 2.97$ g/cm^3. The reason is that in the two novel allotropes the connection between the tetrahedra is not as regular as in diamond or C_4. Despite the features of corner- and edge-sharing, the tetrahedra are separated by C-C segments (see the white spheres segments in Figs. 1b and 1c), resulting in a lower density.

The cohesive energies follow this trend (last row of Table 1), showing cohesive energies with smaller magnitudes than C_4 with E_{coh}/atom = -2.49 eV. Note that C_{12} with edge sharing tetrahedra is found to be more cohesive than C_9 with a mix of edge- and corner-sharing tetrahedra.

Results and discussions

Charge density projections

To illustrate the effect of tetrahedra stacking on the charge distributions, the projections of the charge densities resulting from the ground state structures were obtained by qualitative graphical analysis and are shown in Fig. 2. In C_4 (Fig. 2a), the sp^3-type hybridization is well illustrated around the body-center and corner atoms. Turning to C_9, which contains both corner- and edge-sharing tetrahedra, the yellow volume charges with tetrahedral shapes are less localized and extend throughout the structure. The effect of edge-sharing tetrahedra in C_{12} is shown by a smeared charge density volumes along the C-C bonds.

Mechanical properties

(i) Elastic constants

The calculated sets of elastic constants C_{ij} are given in Table 2. Template bct C_4 is characterized by large elastic constants close to those of diamond. In C_9, C_{ij} have lower values, and the trend is also observed for C_{12} with the specificity of $C_{33} > C_{11}$, probably due to the absence of the carbon atom at 0,0,0.

All C_{ij} (i=j and i≠j) values are positive and their combinations obey the rules of mechanical stability: C_{ii} (i = 1,3,4,6) > 0; $C_{11} > C_{12}$, $C_{11}+ C_{33} - 2C_{13} > 0$; and $2C_{11} + C_{33} + 2C_{12} + 4C_{13} > 0$. The bulk (*B*) and shear (*G*) moduli were calculated from elastic tensors within the Voigt averaging scheme using ELATE software [18]. The corresponding B_V and G_V values shown in the last columns of Table 2 confirm the trends when comparing the elastic constants: C_4 has the largest bulk and shear moduli, with diamond-like values: B_V =445 GPa, and G_V = 530 GPa [19]. At the same time, C_9 and C_{12} have lower values.

(ii) Hardness

Four modern theoretical models [20-23] have been used to predict (H_V). It has been previously reported that the thermodynamic (T) model [20], which is based on thermodynamic properties and crystal structure, shows surprising agreement with available experimental data [24] and is therefore recommended for hardness evaluation of superhard and ultrahard phases [25]. The Lyakhov-Oganov (LO) model [21] takes into account the topology of the crystal structure, the strength of covalent bonding, the degree of ionicity and directionality; however, in the case of ultrahard phases

of light elements, this model gives underestimated hardness values [24,25]. Empirical models, Mazhnik-Oganov (MO) [22] and Chen-Niu (CN) [23], are based on elastic properties, namely bulk and shear moduli. Fracture toughness (K_{Ic}) was evaluated using the Mazhnik-Oganov model [22]. The results are summarized in Tables 3 and 4.

Table 3 shows the crystal parameters, density and Vickers hardness calculated from the thermodynamic model. For template C_4, all values are close to those of diamond and lonsdaleite, as expected. The hardness of tetragonal C_9 and C_{12} is lower, but in both cases it exceeds 80 GPa, which allows us to assign these allotropes to the family of ultrahard phases [28]. We also calculated hardness of two **sqc** allotropes from the SACADA database, sqc3051 and sqc6952. The hardness values were found to be 51 and 67 GPa, respectively, which is a correlation with the density.

Table 4 shows the hardness values calculated using other models in addition to the thermodynamic model. As in the case of other ultrahard phases [25], the Lyakhov-Oganov model gives underestimated hardness values, while both empirical models do not work properly in the case of C_9 and C_{12}, which are characterized by low (0.82 and 0.71) values of the Pugh's modulus ratio (G/B).

Dynamical stability from the phonons

Further stability criteria can be sought from the phonon dispersion relations in the Brillouin zone (BZ), i.e. with the phonon band structures. The phonon band structures obtained for the three carbon allotropes are shown in Fig. 3. In each panel the bands run along the main lines of the tetragonal BZ.

Along the vertical direction the frequency is given in units of terahertz (THz). Since no negative energy values are observed, the three allotropes are considered to be dynamically stable. There are 3N-3 high-energy optical modes and 3 acoustic modes. The acoustic modes start from zero energy ($\omega = 0$) at the Γ point, BZ-center, up to a few terahertz. These modes correspond to the lattice rigid translation modes of the crystal (two transverse and one longitudinal).

Like C_4, C_9 and C_{12} exhibit high-frequency bands in the range of 40 THz. Such a magnitude is a signature observed for diamond by Raman spectroscopy [29]. It can be suggested that both novel C_9 and C_{12} are expected to be dynamically close to diamond.

Thermodynamic properties

The thermodynamic properties were calculated from the phonon frequencies using the statistical thermodynamic expressions on a high precision sampling mesh in the Brillouin zone [30]. For all three allotropes, C_4, C_9 and C_{12}, the temperature dependencies of the heat capacity at constant volume (C_V) are shown in Fig. 4 in comparison with experimental values for diamond [31,32]. The curves corresponding to the temperature change of the entropy S are also shown. The nearly linear increase in entropy with temperature is expected as a signature of increased disorder within the lattice. The $C_V = f(T)$ curve of C_4 in Fig. 4a exactly follows the evolution of the diamond

experimental points, but a relatively small deviation in magnitude can be observed for the calculated $C_V = f(T)$ curves of C_9 and C_{12}. However, a better agreement with the diamond experimental points can be observed for C_{12}. It can be proposed that although the novel allotropes are structurally different from diamond, especially with respect to the stacking of tetrahedra, they remain close to it dynamically and thermally.

Electron band structures

The electronic band structures are shown in Fig. 5. Along the x-axis, the bands develop along the main lines of the tetragonal BZ. Along the y-axis, the zero energy is with respect to the top of the valence band (VB), i.e. E_V. Like C_4, both C_9 and C_{12} allotropes are insulating with large band gaps, close to 5 eV. This behavior is an indication of the closeness of these two allotropes to diamond.

Conclusions

In this work we have proposed novel carbon allotropes with tetragonal symmetry: C_9 and C_{12} based on square carbon units and leading to mixed arrangements of corner and edge *C4* tetrahedra. The initial structures, which were subjected to unconstrained geometry optimization within density functional theory, resulted in cohesive stable phases. C_9 and C_{12} were found to be mechanically and dynamically close to diamond and to have similar thermal properties. The electronic band structures show insulating behavior with band gaps close to 5 eV, like diamond.

References

[1] Oganov, A.R. (2018). Crystal structure prediction: reflections on present status and challenges. *Faraday Discuss.* **211**, 643-660.

[2] Hoffmann, R., Kabanov, A.A, Goloy, A.A. & Proserpio, D.M. (2016). Homo Citans and carbon allotropes: For an ethics of citation. *Angew. Chem. Int. Ed.* **55**, 10962–10976; SACADA database **(***Samara Carbon Allotrope Database*). www.sacada.info

[3] Blatov V.A., Shevchenko A.P. & Proserpio D.M. (2014). Applied topological analysis of crystal structures with the program package ToposPro. *Cryst. Growth Des.* **14**, 3576-3586.

[4] Hohenberg, P. & Kohn, W (1964). Inhomogeneous electron gas. *Phys. Rev. B* **136**, 864-871.

[5] Kohn, W. & Sham, L.J. (1965). Self-consistent equations including exchange and correlation effects. *Phys. Rev. A* **140**, 1133-1138.

[6] Matar, S.F. & Solozhenko, V.L. (2022). The simplest dense carbon allotrope: Ultra-hard body centered tetragonal C_4. *J. Solid State Chem*. **314**, 123424; Matar, S.F. & Solozhenko, V.L. (2023). Corrigendum to "The simplest dense carbon allotrope: Ultra-hard body-centered tetragonal C_4". *J. Solid State Chem*. **317**, 123587.

[7] Matar, S.F. & Solozhenko V.L. (2023). Novel ultrahard sp^2 /sp^3 hybrid carbon allotrope from crystal chemistry and first principles: Body-centered tetragonal C_6 ('neoglitter'). *Diam. Relat. Mater.* **133**, 109747.

[8] Kresse, G. & Furthmüller, J. (1996). Efficient iterative schemes for ab initio total-energy calculations using a plane-wave basis set. *Phys. Rev. B* **54**, 11169.

[9] Kresse, G. & Joubert, J (1994). From ultrasoft pseudopotentials to the projector augmented wave. *Phys. Rev. B* **59**, 1758-1775.

[10] P.E. Bloch (1994). Projector augmented wave method. *Phys. Rev. B* **50**, 17953-17979.

[11] Perdew, J., Burke, K. & Ernzerhof, M. (1996). The Generalized Gradient Approximation made simple. *Phys. Rev. Lett.* **77**, 3865-3868.

[12] Voigt, W. (1889). Über die Beziehung zwischen den beiden Elasticitätsconstanten isotroper Körper. *Annal. Phys.* **274**, 573-587.

[13] Togo, A. & Tanaka, I. (2015). First principles phonon calculations in materials science. *Scr. Mater*. **108**, 1-5.

[14] Momma, K. & Izumi, F. (2011). VESTA 3 for three-dimensional visualization of crystal, volumetric and morphology data. *J. Appl. Crystallogr*. **44**, 1272-1276.

[15] Eyert, V. (2000). Basic notions and applications of the augmented spherical wave method. *Int. J. Quantum Chem.* **77**, 1007-1031.

[16] Pophale, R., Cheeseman, P.A., Deem, M.W. (2011). A database of new zeolite-like materials. *Phys. Chem. Chem. Phys.* **13**, 12407-12412.

[17] CCSD - Deposition Number 2246924. Refcode: QIDCOZ. DOI: 10.5517/ccdc.csd.cc2ff3ff & Deposition Number 2248239. Refcode: YICSEM. DOI: 10.5517/ccdc.csd.cc2fggv7

[18] Gaillac, R., Pullumbi, P. & Coudert, F.-X. (2016). ELATE: an open-source online application for analysis and visualization of elastic tensors. *J. Phys.: Condens. Matter* **28**, 275201.

[19] Brazhkin, V. & Solozhenko, V.L. (2019). Myths about new ultrahard phases: Why materials that are significantly superior to diamond in elastic moduli and hardness are impossible. *J. Appl. Phys.* **125**, 130901.

[20] Mukhanov, V.A., Kurakevych, O.O. & Solozhenko V.L. (2008). The interrelation between hardness and compressibility of substances and their structure and thermodynamic properties. *J. Superhard Mater.* **30**, 368-378.

[21] Lyakhov, A.O. & Oganov, A.R. (2011). Evolutionary search for superhard materials: Methodology and applications to forms of carbon and TiO_2. *Phys. Rev. B* **84**, 092103.

[22] Mazhnik, E. & Oganov, A.R. (2019). A model of hardness and fracture toughness of solids. *J. Appl. Phys.*, **126**, 125109

[23] Chen, X.Q., Niu, H., Li, D. & Li, Y. (2011). Modeling hardness of polycrystalline materials and bulk metallic glasses. *Intermetallics*, **19**,1275-1281.

[24] Matar, S.F. & Solozhenko, V.L. (2021). Crystal chemistry and ab initio prediction of ultrahard rhombohedral B_2N_2 and BC_2N. *Solid State Sci.*, **118**, 106667.

[25] Solozhenko, V.L. & Matar, S.F. (2023). Prediction of novel ultrahard phases in the B–C–N system from first principles: Progress and problems. *Materials*, **16**, 886.

[26] Ownby, P.D., Yang, X. & Liu, J. (1992). Calculated X-ray diffraction data for diamond polytypes. *J. Am. Ceram. Soc.*, **75**, 1876-1883.

[27] Bindzus, N., Straasø, T., Wahlberg, N., Becker, J., Bjerg, L., Lock, N., Dippel, A.-C. & Iversen, B.B. (2014). Experimental determination of core electron deformation in diamond. *Acta Cryst. A*, **70**, 39-48.

[28] Solozhenko, V.L. & Le Godec, Y. (2019). A hunt for ultrahard materials. *J. Appl. Phys.*, **126**, 230401.

[29] Krishnan, R.S. (1945). Raman spectrum of diamond. *Nature* **155**, 171.

[30] Dove, M.T. Introduction to lattice dynamics, Cambridge University Press, 1993.

[31] DeSorbo, W. (1953). Specific heat of diamond at low temperatures. *J. Chem. Phys.* **21**, 876-880.

[32] Victor, A.C. (1962). Heat capacity of diamond at high temperatures. *J. Chem. Phys.* **36**, 1903-1911.

Table 1 Crystal structure parameters of tetragonal C_4, C_9 and C_{12}.

	C_4	C_9 4,4,4**T**6902-**HZ**	C_{12} **sqc**5532
a (Å^3)	2.527	3.885	4.598
c (Å^3)	3.574	4.078	3.814
C1 (brown)	(2*a*) 0, 0, 0	(1*a*) 0, 0, 0	(4*h*) 0.33, 0.33; 0
C2 (white)	(2*d*) ½, 0, ¼	(4*j*) 0, 0.295, 0.754	(8*i*) 0.326,0.169,0.354
C3 (green)		(4*i*) 0.297, 0.297, ½	
Cell volume (Å^3)	22.82	61.57	80.62
Density (g/cm^3)	3.50	2.92	2.97
tetrahedra $d_{C1\text{-}C2}$ (Å^3)	1.55	1.52	1.54
$d_{C2\text{-}C2}$ (Å^3)		1.55	1.50
squares $d_{C2\text{-}C2}$ (Å^3)		1.58	1.56
∠C2-C1-C2 (°) ∠C3-C3-C2 (°)	109.47	97.57 90.27 / 138	 90.27 / 139
E_{total} (eV)	-36.36	-75.51	-102.29
E_{coh}/atom (eV)	-2.49	-1.80	-1.92

Table 2 Elastic constants C_{ij} and Voigt values of bulk (B_V) and shear (G_V) moduli (all values are in GPa) of tetragonal C_4, C_9 and C_{12}.

	C_{11}	C_{12}	C_{13}	C_{33}	C_{44}	C_{66}	B_V	G_V
C_4	1147	28	126	1050	461	559	434	520
C_9	777	95	159	547	316	225	325	266
C_{12}	598	149	162	850	197	231	332	237

Table 3 Tetragonal C_4, C_9 and C_{12}: lattice parameters, density (ρ), Vickers hardness (H_V) and bulk moduli (B_0) calculated in the framework of thermodynamic model of hardness [20]

	Space group	$a = b$ (Å)	c (Å)	ρ (g/cm^3)	H_V (GPa)	B_0 (GPa)
C_4 [#119]	*I*-4*m*2	2.5271	3.5740	3.496	97	440
C_9 [#115]	*P*-4*m*2	3.8855	4.0784	2.915	81	367
C_{12} [#115]	*P*-4*m*2	4.5977	3.8137	2.969	82	374
sqc3051 [#131]	$P4_2/mmc$	3.7966	8.9542	1.854	51	233
sqc6952 [#123]	*P*4/*mmm*	5.2802	4.2498	2.693	67	311
Lonsdaleite	$P6_3/mmc$	2.5221*	4.1186*	3.516	97	443
Diamond	*Fd*-3*m*	3.56661†		3.517	98	445‡

* Ref. 26

† Ref. 27

‡ Ref. 19

Table 4 Mechanical properties of carbon allotropes: Vickers hardness (H_V), bulk modulus (B), shear modulus (G), Young's modulus (E), Poisson's ratio (ν) and fracture toughness (K_{Ic})

	H_V				B		G_V	E**	ν**	K_{Ic}‡
	T*	LO†	MO‡	CN§	B_0*	B_V				
	GPa									MPa·m$^{1/2}$
C_4 #119	97	89	98	93	440	434	520	1115	0.072	6.2
C_9 #115	81	68	37	38	367	325	266	627	0.179	5.1
C_{12} #115	82	75	28	30	374	332	237	574	0.212	4.7
Lonsdaleite	97	90	99	94	443	432	521	1115	0.070	6.2
Diamond	98	90	100	93	445††		530††	1138	0.074	6.4

* Thermodynamic model [20]

† Lyakhov-Oganov model [21]

‡ Mazhnik-Oganov model [22]

§ Chen-Niu model [23]

** E and ν values calculated using isotropic approximation

†† Ref. 19

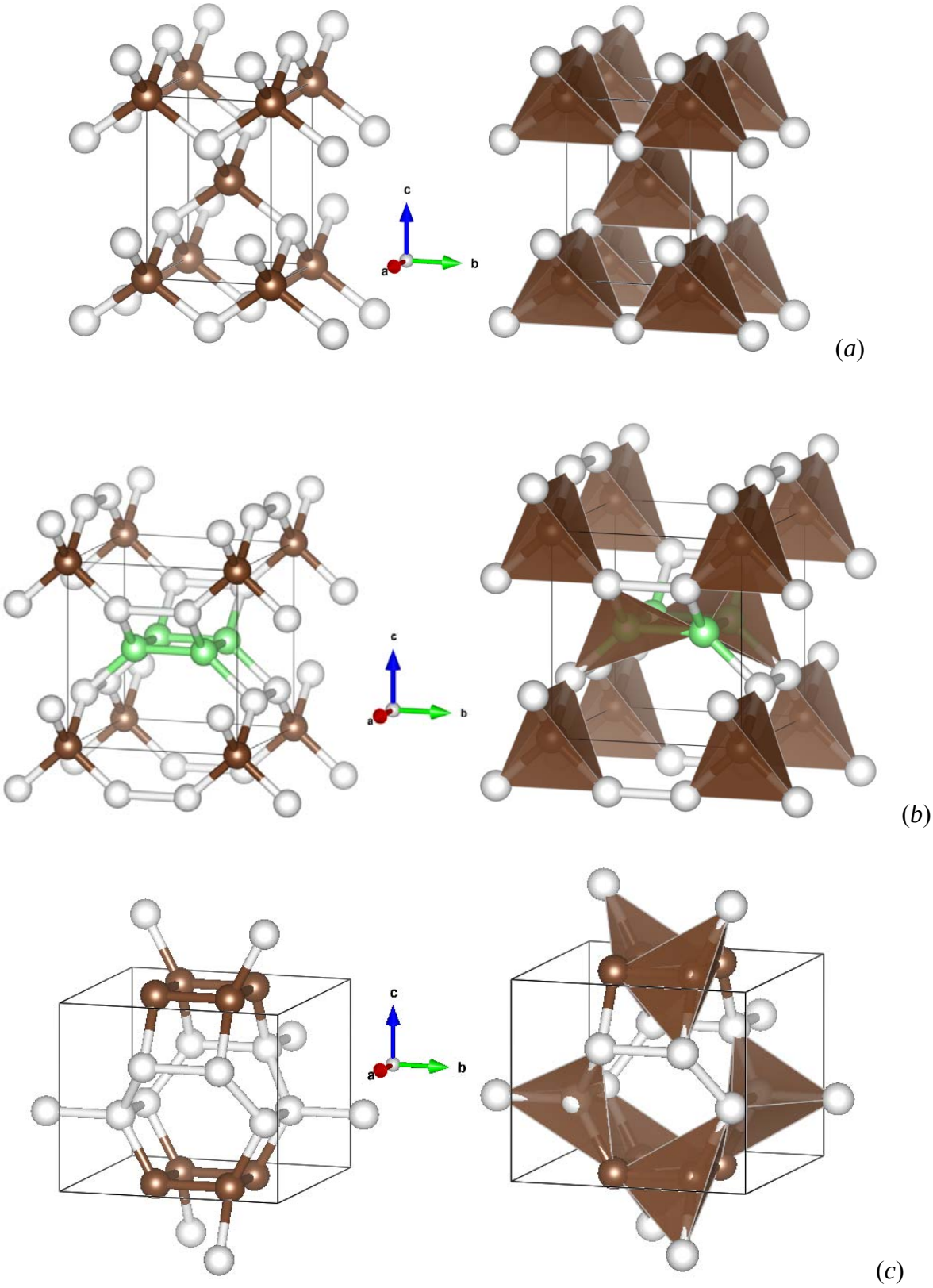

Fig. 1. Structural sketches of the tetragonal C_4 (*a*), C_9 (*b*) and C_{12} (*c*) with ball-and-stick (left) and tetrahedral (right) representations. The colored spheres show the carbon atoms belonging to different lattice sites (see Table 1)

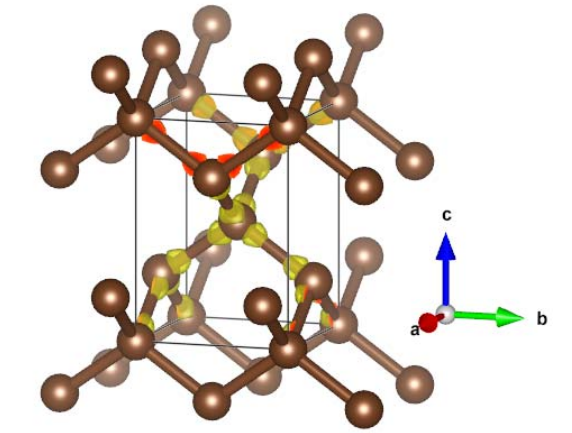

(*a*)

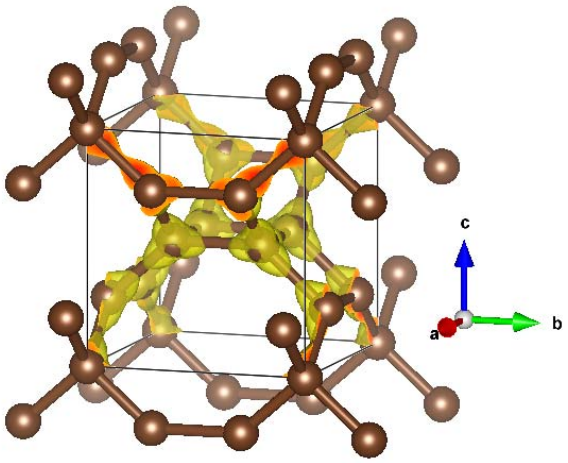

(*b*)

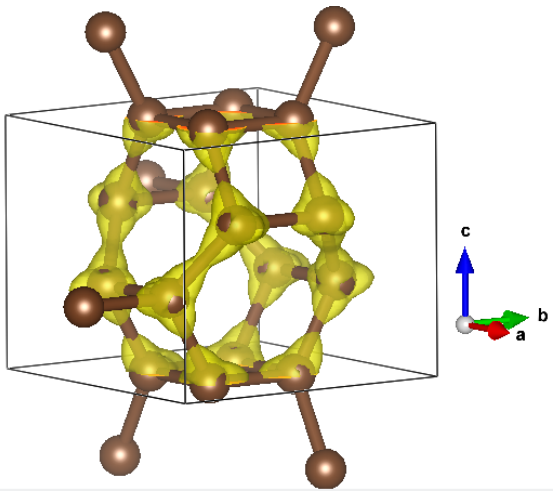

(*c*)

Fig. 2. Charge density yellow volumes in tetragonal C_4 (*a*), C_9 (*b*) and C_{12} (*c*).

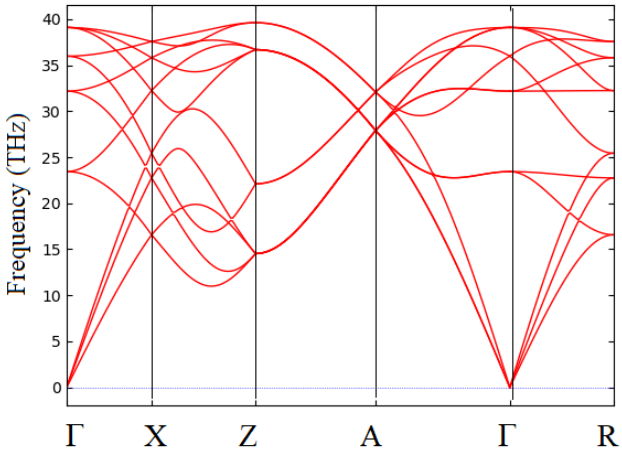

(*a*)

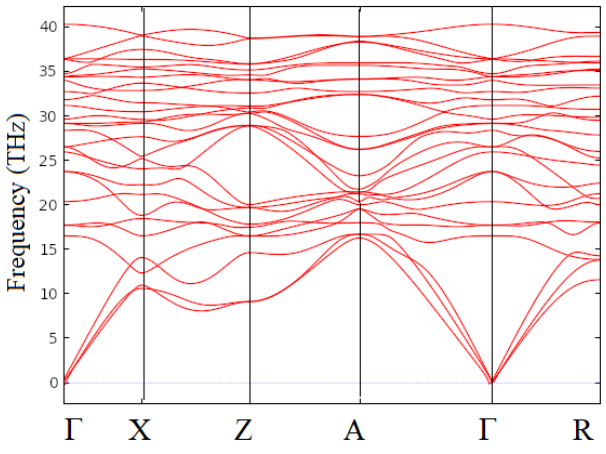

(*b*)

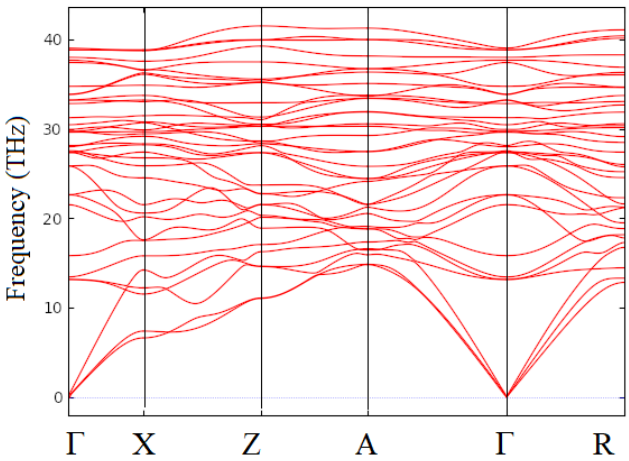

(*c*)

Fig. 3. Phonons band structure of tetragonal C_4 (*a*), C_9 (*b*) and C_{12} (*c*).

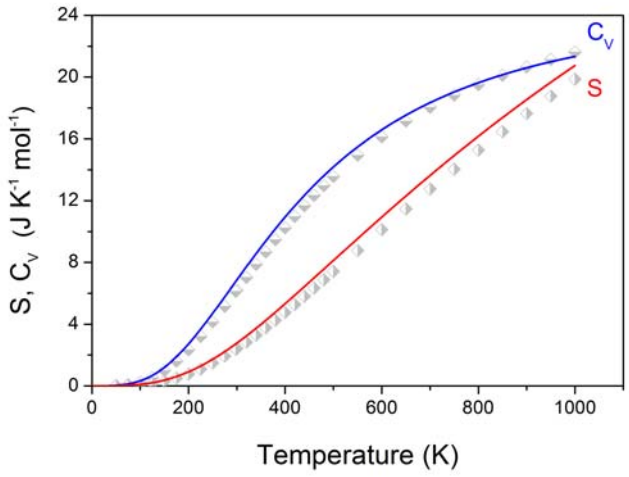

(*a*)

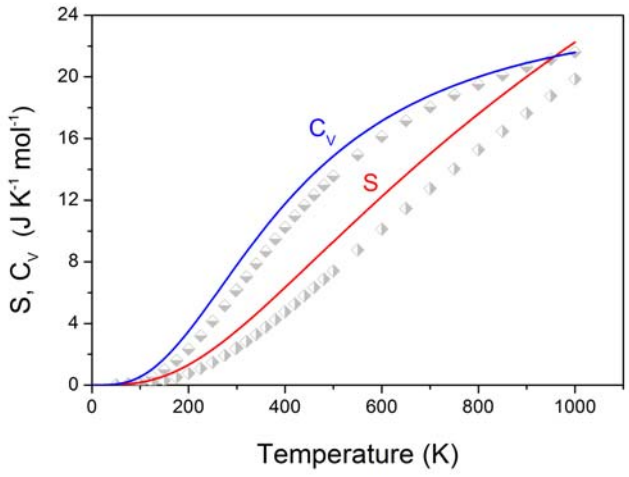

(*b*)

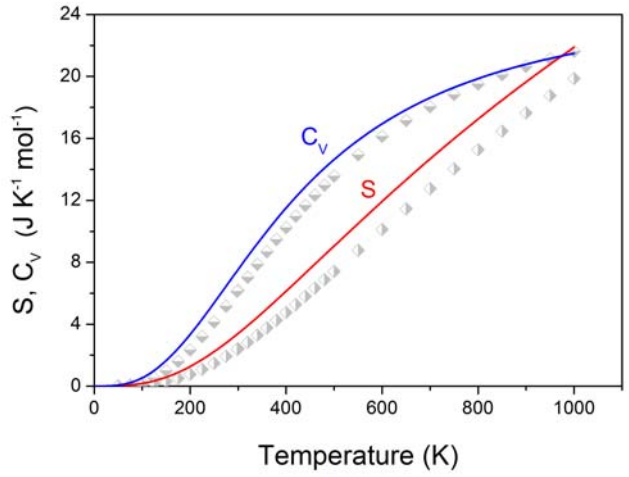

(*c*)

Fig. 4. Heat capacity at constant volume and entropy of tetragonal C_4 (*a*), C_9 (*b*) and C_{12} (*c*) as functions of temperature. Corresponding data for diamond [31,32] are shown as gray symbols.

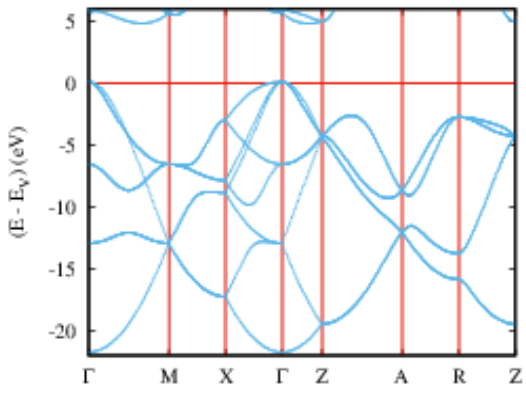

(*a*)

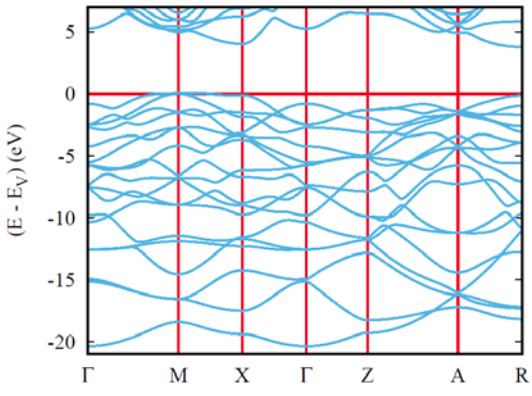

(*b*)

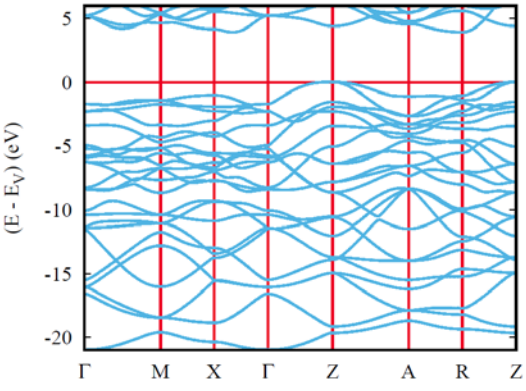

(*c*)

Fig. 5. Electronic band structures of tetragonal C_4 (*a*), C_9 (*b*) and C_{12} (*c*).